Available online at www.sciencedirect.com
ScienceDirect
Nuclear Physics B (Proc. Suppl.) 198 (2010) 75–83
NUCLEAR PHYSICS B PROCEEDINGS SUPPLEMENTS
www.elsevier.com/locate/npbps

HERA results and their impact for LHC

N. Raičević (on behalf of the H1 and ZEUS Collaborations) [a]

[a]University of Montenegro, Faculty of Science, Džorža Vašingtona BB, 20000 Podgorica, Montenegro

This paper is focused on recent results on inclusive measurements and determination of parton density functions from HERA and their impact for LHC.

1. Introduction

In pp collisions at high energy, as planned at the LHC, the final state is produced from interaction of partons from the colliding protons. According to the factorization theorem [1], a cross section involving hadrons can be decomposed into a short distance part and a long distance part. The short distance or hard scattering part can be calculated perturbatively using the (ultraviolet) renormalisable theory of QCD. The long distance part involves the parton density functions (PDFs), into which the infrared divergences of QCD are absorbed. The PDFs, which are probability densities of partons existing inside the proton, need to be extracted from experimental data. Deep inelastic scattering (DIS) is considered as one of the best tools for the determination of PDFs.

The H1 and ZEUS experiments at the HERA collider study $e^{\pm}p$ DIS processes in detail and extract PDFs with high precision as will be discussed in this paper.

The kinematics of inclusive deep inelastic electron[1]-proton scattering is described in terms of the variables Q^2, the four-momentum transfer squared of the exchanged vector boson, Bjorken x, the fraction of the momentum of the incoming nucleon carried by the struck quark, and inelasticity $y = Q^2/sx$, which is a measure of the energy transferred between the electron and the proton. The centre of mass energy squared, s, is given by the electron and the proton beam energies, $s = 4E_eE_p$. The neutral current (NC) cross section is defined by three proton structure functions, F_2, F_L and xF_3 as

$$\frac{d^2\sigma(e^{\pm}p \to e^{\pm}X)}{dxdQ^2} = \frac{2\pi\alpha^2}{xQ^4} Y_+(F_2 \mp \frac{Y_-}{Y_+}xF_3 - \frac{y^2}{Y_+}F_L),$$

with $Y_{\pm} = 1 \pm (1 - y^2)$. The part in brackets, depending on structure functions, is called NC reduced cross section. In the framework of the perturbative QCD inspired quark parton model, the structure functions can be directly related to the PDFs. At low Q^2, F_2 is the dominant contribution to the cross section which is an electric-charge squared weighted sum of all flavor quark and anti-quark PDFs. In the low x region, F_2 is dominated by sea-quark PDFs, and the DGLAP [2] evolution of QCD ascribes the Q^2 dependence of F_2 ("scaling violation") originating from gluon splitting into $q\overline{q}$ pairs. HERA experiments provide crucial information on the low x sea-quark and gluon PDFs. At large values of Q^2, xF_3 becomes significant, and gives information on the valence quark distributions, $u_v = u - \overline{u}$ and $d_v = d - \overline{d}$. The structure function F_L is zero in the quark-parton model, i.e., without QCD, but in leading order QCD, a finite value of F_L is expected in the low x region which is directly related to the gluon PDF.

The cross sections of the charged current (CC) DIS interaction, e^+ (e^-) + p $\to \overline{\nu}(\nu) + X$, can be

[1]The term electron is used to denote both electrons and positrons.

doi:10.1016/j.nuclphysbps.2009.12.016

written as

$$\frac{d^2\sigma(e^+p)}{dxdQ^2} = \frac{{G_F}^2}{2\pi} \frac{{M_W}^4}{({Q^2+M_W}^2)^2} \times [\overline{u}+\overline{c}+(1-y)^2(d+s)],$$

$$\frac{d^2\sigma(e^-p)}{dxdQ^2} = \frac{{G_F}^2}{2\pi} \frac{{M_W}^4}{({Q^2+M_W}^2)^2} \times [u+c+(1-y)^2(\overline{d}+\overline{s})],$$

thus bringing flavor sensitivity of the valence quark PDFs at large x.

About 100 (20) pb^{-1} of e$^+$p (e$^-$p) data were collected at HERA until the year 2000 (HERA-I). Afterwards, HERA underwent a major upgrade (HERA-II) aiming for higher luminosity, and until March 2007, HERA provided in total about 500 pb^{-1} of e$^\pm$ p collisions per experiment to H1 and ZEUS.

The increased statistics provides an increased sensitivity to the PDFs at large x and large Q^2, in regions where the precisions of the HERA-I measurements are still statistically limited. In addition, the precision of the structure function measurements by tagging heavy quarks in the final state can be significantly improved by making use of the increased statistics of HERA-II and also the increased capability of heavy quark identification with newly installed tracking devices. During March to June in the year 2007, HERA made a series of dedicated runs with reduced proton beam energies of 460 and 575 GeV as compared to the nominal one 920 GeV. These data sets are important for the direct measurement of F_L, as they allow access to different y for the same (x, Q^2).

Figure 1 shows the kinematic plane in x and Q^2 covered by the HERA experiments together with the domain probed at LHC. In this figure y represents rapidity, not inelasticity. HERA allows for the first time the study of the proton structure in the perturbative domain at very low x, down to 10^{-5}. This regime is particularly important for LHC physics, since the production of particles with masses of about a few hundred GeV's may involve partons at low x. Since the DGLAP equations describe how quark and gluon distribution

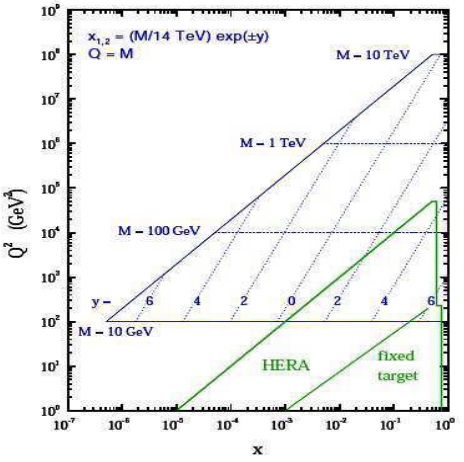

Figure 1. The kinematic plane $x - Q^2$ covered by the HERA experiments together with the domain probed at LHC.

functions evolve with the scale of the interactions, Q^2, particle production in the central rapidity region of the LHC can be predicted using the PDFs measured at the same x at HERA.

2. HERA-I measurements

A new measurement of the inclusive NC e$^+$p DIS cross section is obtained by the H1 Collaboration in the region 12 GeV$\leq Q^2 \leq$ 150 GeV^2 and $2 \cdot 10^{-4} \leq x \leq 0.1$ [3]. The results are based on data collected in the year 2000 and combined with previously published data from HERA-I. The accuracy of the combined measurement is typically in the range of $1.3 - 2\%$. Figure 2 shows the structure function F_2 at fixed Q^2 as a function of x together with H1 data from lower [4] and higher Q^2 [5]. The rise of F_2 when $x \to 0$ is established at very high accuracy. The data are well described by the newest NLO QCD fit from H1 discussed below.

The NC cross section measurements presented in Figure 2, together with the new measurements at lower Q^2 [4] and the previously published H1 NC and CC data provide an accurate H1 data set for the determination of the PDFs. A new QCD analysis, referred to as H1PDF 2009, is performed [3], which uses a general-mass variable flavour number scheme treatment of the

heavy quarks [6]. The general approach to determine the PDFs from experimental DIS cross sections measurements consists of several steps. First, PDFs are parameterized at a low starting scale ${Q_0}^2$ by smooth analytical functions with few free parameters. After this, these functions are evolved using the DGLAP equations to higher Q^2 values and the structure functions and the cross sections are calculated. The calculation is compared to experimental data and a minimisation of the χ^2 is performed by adjusting the free parameters. Several constraints can be applied, like momentum sum rules, requiring the known quark flavor numbers of the proton and possibly a few more. The H1PDF 2009 are parameterized at a starting scale of ${Q_0}^2 = 1.9\ \mathrm{GeV}^2$. Figure 3 shows H1PDF 2009 distributions at $Q^2 = 10\ \mathrm{GeV}^2$ for the valence distributions for up and down quarks as well as the gluon and sea-quark distributions. The gluon and sea quark (xg and xS) are the dominant parton distributions at low x and are determined with high accuracy due to the high precision of the F_2 measurement. As can be seen from the figure, the PDF parameterisation uncertainty, resulting from the parameterization choice, dominates the high x region and the valence distributions, while the low x region is dominated by the model uncertainties which are obtained by varying: the charm mass, the bottom mass, the strange fraction, the minimum Q^2 used in the fit and the starting scale ${Q_0}^2$. The resulting model uncertainty at low x is dominated by the sensitivity of the fit to the ${Q_0}^2$ variation.

The cross section measurements are generally affected by statistical and systematic uncertainties. Both H1 and ZEUS data sets have small statistical errors, thus the systematic uncertainties become increasingly important and their proper treatment essential. The HERA experiments improved this situation by averaging all inclusive H1 and ZEUS HERA-I published results in a model-independent way prior to performing a QCD analysis on them [7]. Since both experiments measure the same cross section at a given kinematic point, the combination procedure is a χ^2 minimization in which the parameters are the true values of the cross section at each (x, Q^2) point and the correlated systematic error parameters [8]. For

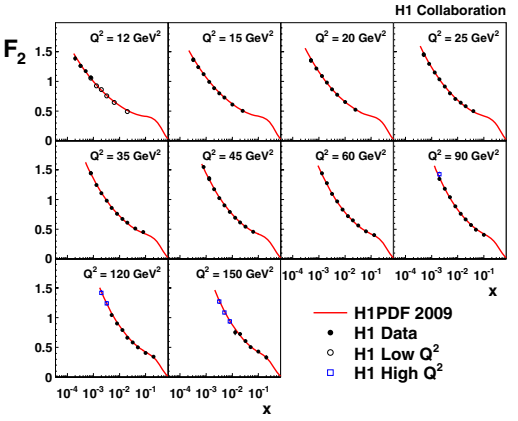

Figure 2. Measurement of the structure function F_2 at fixed Q^2 as a function of x. The error bars represent the total measurement uncertainties. The curve shows the QCD fit described in the text.

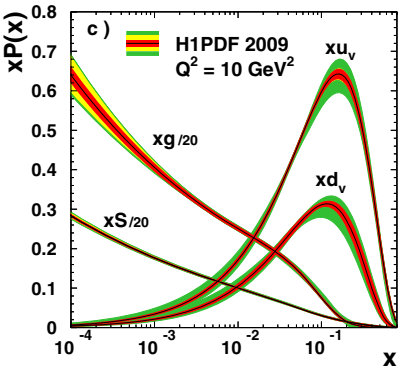

Figure 3. Parton distributions as determined by the H1PDF 2009 QCD fit at $Q^2 = 10\ \mathrm{GeV}^2$. The gluon and sea-quark densities are scaled down by a factor 0.05. The inner error bands show the experimental uncertainty, the middle error bands include the theoretical model uncertainties of the fit assumptions, and the outer error bands represent the total uncertainty including the parameterization uncertainty.

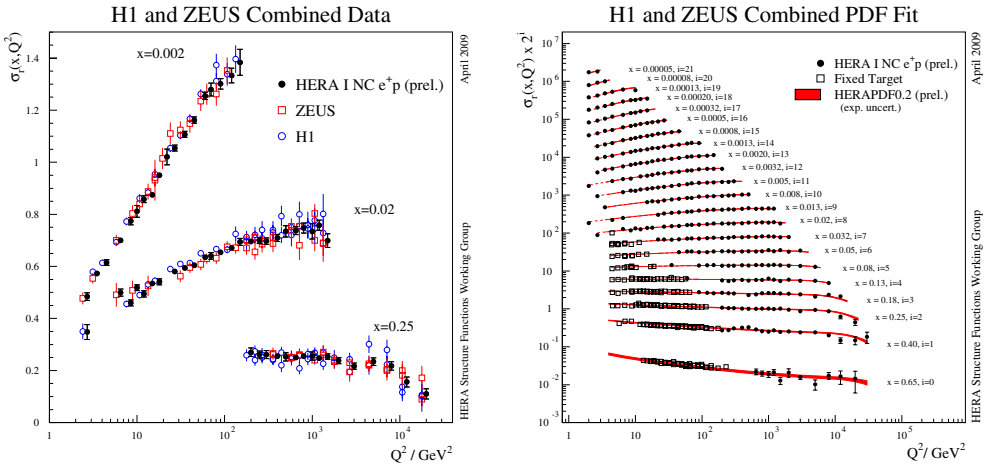

Figure 4. Left: Examples of NC reduced cross section combinations for three bins in x as a function of Q^2, for H1 and ZEUS and combined experimental points. Right: The combined HERA-I NC reduced cross section compared with the HERAPDF0.2. Both data and fit include the experimental errors.

each measurement point a given correlated uncertainty of one data set of measurements is constrained by the independent measurements from other data sets. Such cross-calibration leads to a precise and coherent data set to be used for the determination of the PDFs.

In the χ^2 minimization procedure the uncertainties can be treated as absolute (additive), so they do not depend on the central value of the measurement, or relative (multiplicative). Normalization uncertainties, like the luminosity uncertainty, are relative, but for other systematic uncertainties the situation is not so clear. To estimate the sensitivity of the average to this issue, various different treatments of the systematic uncertainties are considered. The extreme assumptions treat all uncertainties as multiplicative, or all as additive, apart from the normalization uncertainties. An additional systematic uncertainty is estimated based on the difference between these two error treatments. The typical size of this uncertainty is less than 0.5%. 110 systematic sources from the individual experiments and 3 from the combining procedure are considered. This yields a good quality of the fit with $\chi^2/dof = 637/656$.

Figure 4 (left) illustrates the H1 and ZEUS combined cross sections for three selected x bins as a function of Q^2. The individual H1 and ZEUS measurements are compared to the H1 and ZEUS combined measurements. The error bars show the total uncertainty. At low Q^2 where the measurements are limited by systematic uncertainties, the improvement in the total error is significant. At higher Q^2 the combined measurements have smaller uncertainties as compared to the individual data due to the increased statistics. In the region $3 \leq Q^2 \leq 500$ GeV^2, 2% precision for the combined data is obtained, while in the region $20 \leq Q^2 \leq 100$ GeV^2, 1% precision is reached.

Figure 4 (right) shows the combined HERA-I NC reduced cross section measurements as a function of Q^2 for various x bins in the extended kinematic range. The measurements are compared to the fixed target measurements and to the fit corresponding to the complete inclusive HERA-I data, the HERAPDF0.2, discussed below. The impressive precision of the combined data is reflected in the precision of the fit. Extrapolated to lower Q^2, the fit is found to be in very good agreement with the fixed target data.

PDFs are usually determined in global QCD

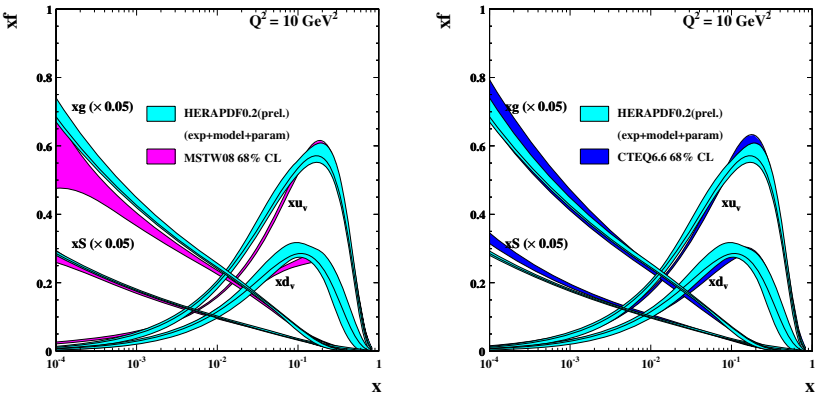

Figure 5. HERAPDF0.2 fit compared with MSTW (left) and CTEQ (right) fits at $Q^2 = 10$ GeV^2.

analysis of DIS data, both from HERA and fixed-target experiments, and also jet production data from TEVATRON [9,10]. Since high Q^2 data became available with high statistics, H1 and ZEUS used their own data alone to make QCD fits and extract PDFs [5,11,3]. Based on the combined HERA-I dataset of $e^{\pm}p$ NC and CC cross sections presented above, a new NLO QCD fit, HERAPDF0.2, was performed [7]. The HERAPDF0.2 distributions are parameterized at ${Q_0}^2 = 1.9$ GeV^2 with 10 free parameters. The χ^2 per degree of freedom of the fit was 576/592.

Figure 5 shows the comparison between the global fits from the MSTW (left) [9] and CTEQ (right) [10] groups and HERAPDF0.2 at $Q^2 = 10$ GeV^2. The global fit distributions are shown at 68% confidence level. The experimental uncertainties of the HERAPDF0.2 are evaluated at 68% confidence level and model and parameterization uncertainties are added. The PDF sets shown are gluon, sea and valence distributions for up and down quarks. The global fits involve data from a much larger variety of experiments and physics processes and thus are forced to use a different error definition than the $\Delta\chi^2 = 1$ criterion applicable to the HERA data alone. The MSTW and CTEQ groups do not evaluate model and parameterization uncertainties explicitly. The precision of the new data lead to precise PDFs, in particular at low x, where most of the cross-calibration that occurs during the averaging procedure significantly improves the systematic errors of the obtained cross sections.

3. Further improvements from HERA-II

The high-statistics HERA-II data will provide a significant improvement of the measurements of CC and NC cross sections at high Q^2, and thus further improvements are foreseen for valence quark PDFs at large x, in particular for the d quark PDF which will be constrained by the e^+p CC data. As shown in the ZEUS-JETS fit [11], the medium and high x region ($0.04 < x < 0.1$) also profits from measurements of jets which have not been included in the combination of data sets.

A measurement of the gluon density at small x, which is not obtained from the scaling violations of F_2, can provide the possibility to investigate the region where the theoretical formalism of the NLO DGLAP equations may need an extension to account for low-x resummation. Such measurements are measurement of F_L which is directly related to the gluon, or measurements of ${F_2}^{c\bar{c}}$ and ${F_2}^{b\bar{b}}$ since the heavy quarks are not ordinary constituents in the proton but are produced from the gluon density of the proton.

Measurement of CC and NC cross sections at high Q^2. Both collaborations, H1 and ZEUS, have published or preliminary measurements from $e^{\pm}p$ interactions on CC and NC cross

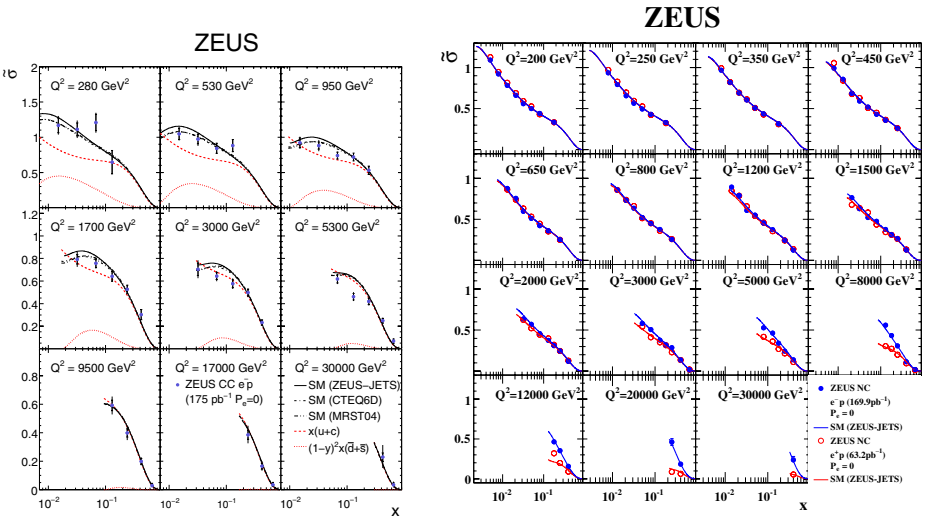

Figure 6. The e^-p CC DIS cross section (left) and the $e^{\pm}p$ unpolarized NC DIS cross section (right) plotted as a function of x at fixed Q^2.

sections from HERA-II data. The ZEUS Collaboration recently published measurements of the cross sections for CC DIS in e^-p collisions with longitudinally polarized electron beams using the whole available statistics from HERA − II data (175 pb^{-1}) in the region $280 < Q^2 < 30000$ GeV^2 and $0.015 < x < 0.65$ [12]. The cross section measurement in this kinematic range is shown in figure 6. The data points were corrected to the unpolarized cross section ($P_e = 0$) using the Standard Model (SM) prediction. The prediction of the SM evaluated using the ZEUS-JETS, CTEQ and MRST PDFs give a good description of the data. The contributions from the PDF combinations $(u + c)$ and $(\overline{d} + \overline{s})$, obtained in the MS scheme from the ZEUS-JETS fit, are shown separately and demonstrate the sensitivity to $(u+c)$. ZEUS also has published a new measurement of the NC cross section for DIS in e^-p collisions with a longitudinally polarized electron beam [13]. The measurements are based on an integrated luminosity of 169 pb^{-1}. The reduced cross sections of unpolarized e^-p NC DIS are presented in figure 6 with the residual polarization of -0.03 corrected using theoretical predictions. The SM predictions are in good agreement with the measurements over the full kinematic range. Also shown are unpolarized e^+p NC DIS measurements with an integrated luminosity of 63.2 pb^{-1} collected in 1999 and 2000 [14]. The total systematic uncertainties for most of the phase space used in the reduced cross section measurements are below 2%.

Structure function xF_3. The difference of the NC cross sections between e^+p and e^-p collision data determines xF_3. At HERA, xF_3 is, to a very good approximation, dominated only by the $\gamma - Z$ interference term, $xF_3{}^{\gamma Z}$, which is determined by the valence quark PDFs and predicted to be only very weakly depending on Q^2. H1 and ZEUS have combined their data to obtain more precise measurement of xF_3 [15] based on an integrated luminosity of 489 pb^{-1} which is about one half of the available statistics. With the new e^-p NC reduced cross section, ZEUS updated their xF_3 measurement [13].

Jet cross section data. The H1 Collaboration has published a new measurement on inclusive jet, 2-jet and 3-jet cross sections from $e^{\pm}p$ scattering at large Q^2, $150 < Q^2 < 15000$ GeV^2 using HERA-I and HERA-II data, corresponding to an integrated luminosity of 395 pb^{-1} [16]. The measurements are well described by perturbative QCD calculations at next-to-leading order

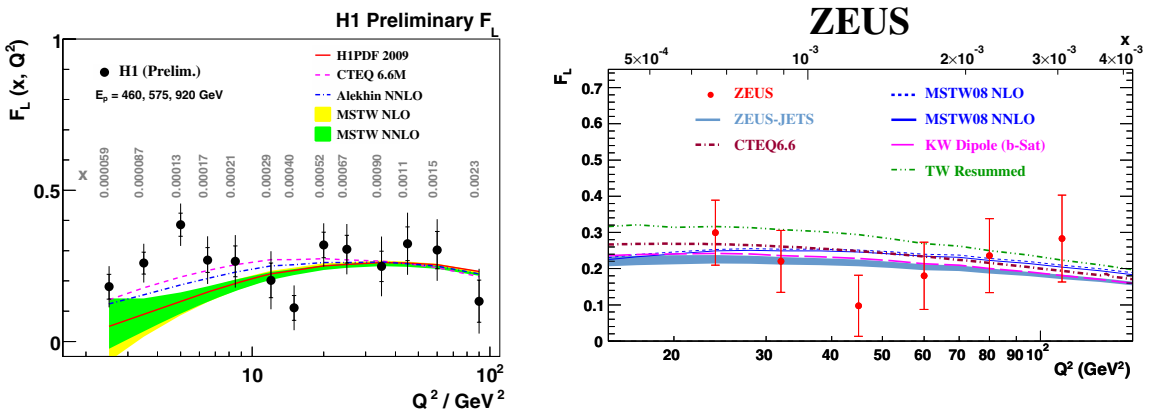

Figure 7. Measurement of the longitudinal structure function F_L at H1 (left) and ZEUS (right).

corrected for hadronization effects. The strong coupling as determined from these measurements is $\alpha_s(M_Z) = 0.1168 \pm 0.0007(\text{exp.})^{+0.0046}_{-0.0030}(\text{th.}) \pm 0.0016(\text{pdf})$.

Measurement of the longitudinal proton structure function. The H1 and ZEUS Collaborations have published measurements of the longitudinal structure function F_L at medium Q^2 determined from NC cross sections at three different centre-of-mass energies, 318, 251 and 225 GeV [17,18]. Published F_L from H1 is measured in the region $2.4 \cdot 10^{-4} < x < 0.0036$ and $12 < Q^2 < 90$ GeV^2, while ZEUS published their measurement in the region $5 \cdot 10^{-4} < x < 0.007$ and $20 < Q^2 < 130$ GeV^2. H1 extended their measurements to low [20] and high Q^2 [19] covering $2.5 \leq Q^2 \leq 800$ GeV^2 and x between 0.00005 and 0.035. The values of F_L resulting from averages over x at fixed Q^2 are presented in Figure 7. The left plot shows results from H1 and the right one from ZEUS compared with predictions based on the fits to their data alone (H1PDF 2009 and ZEUS-JETS), to CTEQ6.6 [10] NLO and MSTW08 [9] NLO and NNLO fits. H1 compares also with prediction from Alekhin fit at NNLO [21]. All these predictions are based on the DGLAP formalism. Also shown are predictions from the NLL BFKL resummation fit from Thorne and White (TW) [22] and the prediction from the impact-parameter-dependent dipole saturation model [23] of Kowalski and Watt based on DGLAP evolution of the gluon density. All of the models are consistent with the data above 10 GeV^2 (H1) and 24 GeV^2 (ZEUS). For $Q^2 < 10$ GeV^2 there is a large spread between the models and the data agree better with CTEQ and Alekhin predictions compared to MSTW and H1PDF 2009. H1PDF 2009 and MSTW use the same code to extract F_L and underestimate the data. The difference between NLO DGLAP models can be understood as an effect of higher order corrections since the MSTW fit uses terms sub-leading in α_s for calculation of F_L which turn out to be negative at NLO.

Measurement of the charm and beauty. The heavy quarks are not ordinary constituents in the proton but are produced from the gluon density of the proton. The prediction of the 'standard' QCD processes at the LHC, such as the inclusive production of W and Z bosons, are sensitive to the theoretical treatment of heavy quarks. The b quark contribution is considered as important in Higgs production at the LHC.

H1 recently published results on inclusive charm and beauty cross sections [24] measured in e^-p and e^+p NC interactions in the kinematic region $5 \leq Q^2 \leq 2000$ GeV^2 and $0.0002 \leq x \leq 0.05$. The analyzed data correspond to an integral luminosity of 189 pb^{-1}. The charm and beauty events are identified using variables reconstructed by the H1 vertex detector including the impact parameter of tracks to the primary vertex and

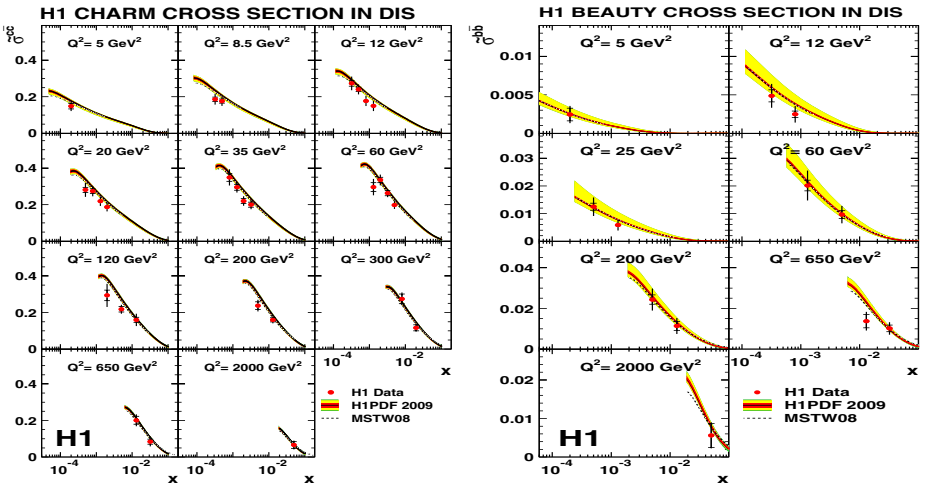

Figure 8. Inclusive charm (left) and beauty (right) cross section as a function of x for different Q^2 values.

the position of the secondary vertex. The results on inclusive charm and beauty cross sections with the predictions from H1 and MSTW at NLO are shown in Figure 8. Both predictions provide a reasonable description of the data.

ZEUS Collaboration also published the new results on charm and beauty production [25] for $Q^2 > 20$ GeV^2.

4. Summary

The combined HERA-I data set, of neutral and charged current inclusive cross sections for e^+p and e^-p scattering, has been used as the input for a NLO QCD fit in the DGLAP formalism. The resulting PDFs are determined with significantly reduced experimental uncertainties compared to the separate analysis of the H1 and ZEUS experiments. The PDF precision is essential for estimation of the cross sections relevant for LHC. Final publications based on the complete HERA data will come in the next years.

REFERENCES

1. J. C. Collins, D. E. Soper, G. Sterman, Adv. Ser. Direct. High Energy Phys., volume 5 (1988) 1; hep-ph/0409313.
2. V .N. Gribov and L. N. Lipatov, Sov. J. Nucl. Phys. 15 (1972) 438; V. N. Gribov and L. N. Lipatov, Sov. J. Nucl. Phys. 15 (1972) 675; Y. L. Dokshitzer, Sov. Phys. JETP 46, (1977) 641; G. Altarelli and G. Parisi, Nucl. Phys. B 126 (1977) 298.
3. F. D. Aaron *et al.*, H1 Collaboration, arxiv:0904.3513.
4. F .D. Aaron *et al.*, H1 Collaboration, arxiv:0904.0929.
5. C. Adloff *et al.*, H1 Collaboration, Eur. Phys. J C 30 (2003) 1.
6. R. S. Thorne and R. G Roberts, Phys. Rev. D 57 (1998) 6871.
7. H1 and ZEUS Collaborations, H1prelim-09-045 and ZEUS-prel- 09-011.
8. A. Glazov, AIP Conf. Proc. 792 (2005) 237.
9. A. D. Martin, W. J. Stirling, R. S. Thorne and G. Watt, Phys. Lett. B 652, (2007) 292.
10. P. M. Nadolsky *et al.*, Phys. Rev. D 78 (2008) 013004.
11. S. Chekanov *et al.*, ZEUS Collaboration, Eur. Phys. J C 42 (2005) 1.
12. S. Chekanov *et al.*, ZEUS Collaboration, Eur. Phys. J C 61 (2009) 223.
13. S. Chekanov *et al.*, ZEUS Collaboration, Eur. Phys. J C 62 (2009) 625.
14. S. Chekanov *et al.*, ZEUS Collaboration, Phys. Rev. D 70 (2004) 052001.
15. H1 and ZEUS Collaborations, H1prelim-06-

142, ZEUS-prel-06-022.
16. F. D. Aaron *et al.*, H1 Collaboration, arxiv:0904.3870.
17. F.D. Aaron *et al.*, H1 Collaboration, Phys. Lett. B 665 (2008) 139.
18. S. Chekanov *et al.*, ZEUS Collaboration, arXiv:0904.1092.
19. H1 Collaboration, H1prelim-08-042.
20. H1 Collaboration, H1prelim-09-044.
21. S. Alekhin, JETP Lett. 82 (2005) 628.
22. C. D. White and R.S. Thorne, Phys. Rev. D 75 (2007) 034005.
23. G. Watt and H. Kowalski, Phys. Rev D 78 (2008) 014016 .
24. F. D. Aaron *et al.*, H1 Collaboration, arxiv:0907.2643.
25. S. Chekanov *et al.*, ZEUS Collaboration, arXiv:0904.3487.